SOLVING THE TWO-DIMENSIONAL INVERSE FRACTAL PROBLEM WITH THE WAVELET TRANSFORM

ZBIGNIEW R. STRUZIK
Department of Computer Science, University of Amsterdam
Kruislaan 403, 1098 SJ Amsterdam, The Netherlands

Abstract

The methodology of the solution to the inverse fractal problem with wavelet transform[1,2] is extended to two-dimensional self-affine functions. Similarly to the one-dimensional case, the two-dimensional wavelet maxima bifurcation representation used is derived from the continuous wavelet decomposition. It possesses the translational and scale invariance necessary to reveal the invariance of the self-affine fractal. As many fractals are naturally defined on two-dimensions this extension constitutes an important step towards solving the related inverse fractal problem for a variety of fractal types.

1. INTRODUCTION

The initial definition referred to the Hausdorff dimension as the principal feature of a fractal. Soon it became obvious that the world of fractals would be unnecessarily restricted if such a definition were maintained. It is the notion of some sort of similarity in scale which has loosely defined the fractal ever since. We adopted this point of view, and with help of the wavelet transform in providing the amazing ability to unfold objects in scale, we were able to reveal the scale position similarity of self-affine fractals. A properly chosen wavelet transform of a fractal exhibits a characteristic regularity, consistent with the renormalisation properties of the fractal. By unfolding a fractal in the scale domain, it becomes possible to investigate its invariance properties.

Indeed, fractals (in particular self-affine attractors) possess by definition invariance which must be identifiable in the form of some elementary transformations (for example those used to create the fractal object). The problem of recovering these transformations from the fractal object is known as the inverse fractal problem (IFP). The wavelet transform therefore provides the necessary means to make the IFP tractable. The crucial step in this approach consists of the possibility of verification of such a scale-space similarity in terms of invariance with respect to some iterative functions (maps). Contrary to the methods for solving the inverse fractal problem, which use a predefined class of Iterated Function System (IFS) functions[3] to approximate the invariance discussed, the approach we present aims at revealing the renormalisation involved in the creation of the fractal, possibly bearing high relevance to the underlying physical phenomena.

We, therefore, propose the hypothesis[1] that an object can be classified as a pre-fractal if there exists a solution to the related inverse fractal problem; in other words, if a set of construction rules can be found which, ultimately, would fully define the object within the scales where it is observed and which allows arbitrary extrapolation in the scale domain.

The goal of this paper is to extend the scope of the methodology developed in Refs.[1,2] to fractals on two-dimensional support using the example of self-affine multiplicative fractal measures. These can be created with $\mathbf{R}^3 \to \mathbf{R}^3$ iterated functions (maps). Like computer generated fractals, natural fractals have the property that they are created by the same phenomena acting at different scales. These phenomena may however show behaviour ranging from purely stochastic to completely deterministic. Although the focus of this paper is on the deterministic limit, a more general application of the techniques is possible.

2. FRACTAL IFS FUNCTIONS IN TWO DIMENSIONS

In this section we will address relevant facts about self-affine functions over two-dimensional (or fractal $1 < D < 2$) support. Self-affinity is a concept inherent to fractal functions including self-similar sets of functions support as a special case. An *affine transformation* $S : \mathbf{R}^n \to \mathbf{R}^n$ is of the form:

$$S(x) = T(x) + b \;, \tag{1}$$

where T is a linear transformation on $\mathbf{R}^n$ (often represented by an $n \times n$ matrix) and b is a vector in $\mathbf{R}^n$. Therefore, an affine transformation is in general a combination of translation, rotation, dilation and possibly reflection.

Of special relevance to creation of fractal attractors is a *contraction* transformation S:

$$\begin{array}{ll} S : \mathbf{R}^n \to \mathbf{R}^n & \text{is a contraction if there is a number } c \text{ and } 0 < c < 1 \\ \text{such that} & |S(x) - S(y)| \leq c|x - y| \quad \text{for all } x, y \in \mathbf{R}^n. \end{array}$$

Affine transformations, having different contraction ratios in different directions, are to be distinguished from similarities which contract isotropically:

$$\text{if } |S(x) - S(y)| = c|x - y| \text{ for all } x, y \in \mathbf{R}^n \text{ then } S \text{ is a similarity.}$$

For $S_1, ..., S_N$ affine *contractions* on $\mathbf{R}^n$, by the standard result, see e.g. Ref.[4], the unique compact set F invariant with respect to S_n is guaranteed to exist and is termed a *self-affine set* or an *attractor* of $S_n, n = 1, ..., N$. Thus for the self-affine set F obtained by

$$F_k = \left[\bigcup_{n=1}^{N} S_n \right]^{\circ k} (B) \qquad \text{for any } B \in \mathbf{R}^n \;; \qquad F = lim_{k \to \infty} F_k \;, \tag{2}$$

where $\circ$ denotes the composition of transformations, so that

$$(P_1 \circ P_2 \circ ... \circ P_k)(x) = P_1(P_2(...(P_k(x))...)),$$

the following relation is satisfied:

$$F = S_n(F) \qquad \forall S_n, n = 1, ..., N. \tag{3}$$

The subsequent approximations F_k of the set F are called pre-fractals.

We will consider continuous contraction transformations $S_n : \mathbf{R}^3 \to \mathbf{R}^3$, in short to be called *maps*, chosen in such a way that the self-affine set they define is a functional mapping $f : \mathbf{R}^2 \to \mathbf{R}$.

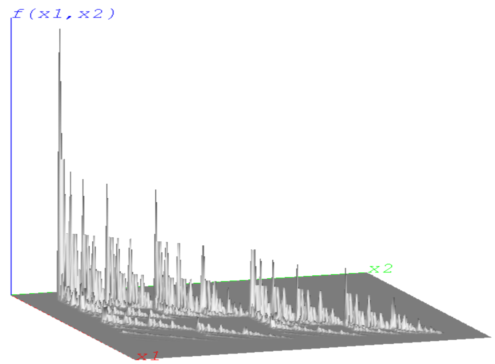

Figure 1: The test case: Sierpiński triangle with non-uniformly distributed measure.

Let S_n $(1 \le n \le N)$ be an affine transformation represented in matrix notation with respect to the coordinates $\{x_1, x_2, y\}$ by

$$S_n \begin{pmatrix} x_1 \\ x_2 \\ y \end{pmatrix} = \begin{pmatrix} a_n & b_n & 0 \\ c_n & d_n & 0 \\ \gamma_{n1} & \gamma_{n2} & \alpha_n \end{pmatrix} \begin{pmatrix} x_1 \\ x_2 \\ y \end{pmatrix} + \begin{pmatrix} e_n \\ f_n \\ \delta_n \end{pmatrix} . \tag{4}$$

For the sub-transformation on the coordinates $\{x_1, x_2\}$:

$$S_{xn} \begin{pmatrix} x_1 \\ x_2 \end{pmatrix} = \begin{pmatrix} a_n & b_n \\ c_n & d_n \end{pmatrix} \begin{pmatrix} x_1 \\ x_2 \end{pmatrix} + \begin{pmatrix} e_n \\ f_n \end{pmatrix} , \tag{5}$$

which describes an arbitrary affine transformation in $\mathbf{R}^2$, we will require

$$0 < \sigma_n^{-1} = \begin{vmatrix} a_n & b_n \\ c_n & d_n \end{vmatrix} < 1 ,$$

which ensures that S_{xn} is a similitude and the transformed surface does not vanish or flip over. We will also restrict S_n to be a set of non-overlapping transformations:

$$\bigcap_n S_n(A) = \emptyset, \;\; \forall A, \;\; \text{where } A \text{ is an arbitrary compact set.}$$

Additional constraints can be specified for the purpose of generating a fractal interpolation surface ensuring joining up of the transformed surfaces at the interpolated points.[*]

[*]These conditions are however irrelevant to this work. In fact, for the sake of simplicity, we will limit ourselves to examples without additional components in the function value which translates to $\gamma_n = 0$ and $\alpha_n = 0$.

3. TWO-DIMENSIONAL WAVELET TRANSFORM ON FRACTAL FUNCTIONS

3.1 The two-dimensional continuous wavelet transform

The (real-valued) wavelet transform W decomposes the function $f(\bar{x}) \in L^2(\mathbf{R}^2)$ in the base of elementary wavelets created by the action of the affine group on a single function $\psi(\bar{x})$ †

$$(Wf)(\bar{\bar{s}}, \bar{b}) = \frac{1}{|\bar{\bar{s}}|} \int d\bar{x}\; f(\bar{x})\; U(\bar{\bar{s}}, \bar{b})\, \psi(\bar{x}) \quad \text{where} \quad U(\bar{\bar{s}}, \bar{b})\psi(\bar{x}) = \psi((\bar{\bar{s}})^{-1}(\bar{x} - \bar{b})). \tag{6}$$

In practice, the wavelet $\psi(\bar{x})$ is chosen to be well localised both in scale and space, and if no directional sensitivity is required uniform scaling in all directions is a natural choice. The matrix $\bar{\bar{s}}$ can be than reduced to two equal scaling factors s on the diagonal and $|\bar{\bar{s}}| = s^2$ ‡

Further, the choice of the analysing wavelet $\psi(\bar{x})$ is dependent on the application. For our purpose, we will need the wavelet with m vanishing moments, that is orthogonal to polynomials of order $l < m$:

$$\int_{-\infty}^{+\infty} \bar{x}^l\, \psi(\bar{x})\, d\bar{x} = 0 \qquad \forall l,\; 0 \le l < m. \tag{7}$$

Arguments for the choice of m will be given in part 4 of the paper.

In this work we use continuous parametrization of the affine operator $U(\bar{\bar{s}}, \bar{b})$ known as continuous wavelet transform (CWT). However, restricting $\bar{\bar{s}}, \bar{b}$ to discrete values gives the discrete wavelet transform which, for the particular choice of a wavelet satisfying the orthogonality criteria, constitutes an important class of orthogonal wavelet transforms.

3.2 The multi-resolution scheme

Since the self-affine attractor is by definition invariant with respect to some affine operator $T(\bar{\bar{u}}, \bar{v})$:

$$f = T(\bar{\bar{u}}, \bar{v})f; \qquad T(\bar{\bar{u}}, \bar{v})(\bar{x}) = \bar{\bar{u}}\bar{x} + \bar{v}, \tag{8}$$

we expect this to be reflected in the invariance of the wavelet transform. Indeed,

$$\begin{aligned} (Wf)(\bar{\bar{s}}, \bar{b}) &= \frac{1}{|\bar{\bar{s}}|} \int d\bar{x}\; f(\bar{x})\; (U(\bar{\bar{s}}, \bar{b})\, \psi(\bar{x})) \\ &= \frac{1}{|\bar{\bar{s}}|} \int d\bar{x}\; (T(\bar{\bar{u}}, v)\; f(\bar{x}))\; (U(\bar{\bar{s}}, \bar{b})\; \psi(\bar{x})) \\ &= \frac{1}{|\bar{\bar{s}}|} \int d\bar{x}\; f(\bar{x})\; (T^\dagger(\bar{\bar{u}}, \bar{v})\; U(\bar{\bar{s}}, \bar{b}))\; (\psi(\bar{x})) \end{aligned} \tag{9}$$

which, using an easily verifiable relation $T^\dagger(\bar{\bar{u}}, \bar{v}) = \frac{1}{|\bar{\bar{u}}|} T^{-1}(\bar{\bar{u}}, \bar{v}) = \frac{1}{|\bar{\bar{u}}|} U(\bar{\bar{u}}, \bar{v})$, where $T^\dagger$ denotes an operator adjoint to T, can be written as:

$$(Wf)(\bar{\bar{s}}, \bar{b}) = \frac{1}{|\bar{\bar{u}}|} \frac{1}{|\bar{\bar{s}}|} \int d\bar{x}\; f(\bar{x})\; (U(\bar{\bar{u}}, \bar{v})\; U(\bar{\bar{s}}, \bar{b}))\; (\psi(\bar{x})). \tag{10}$$

† Formally, the choice of the wavelet $\psi(\bar{x})$ is subject to one restriction: $\psi(\bar{x})$ must be *admissible*, i.e. of zero mean, if the function is to be reconstructed from its wavelet transform. Since we investigate only invariance properties of the functions' wavelet transform, we lift this requirement.

‡ The normalising factor s^2 is taken per default if working in two dimensions. This may need 'correcting' in Eq. (15) using the fractal dimension of the support of the attractor recovered from the solution to the IFP.

One can easily show that the action of $[U(\bar{\bar{u}},\bar{v})]^k\, U(\bar{\bar{s}},\bar{b})$ is equivalent to applying the operator $U(\bar{\bar{s}}^{(k)},\bar{b}^{(k)})$ where k indexes the action of the operator $U(\bar{\bar{u}},\bar{v})$

$$\left\{ \begin{array}{lcl} \bar{\bar{s}}^{(k)} & = & \bar{\bar{u}}^k\, \bar{\bar{s}} \\ \bar{b}^{(k)} & = & \bar{\bar{u}}^k \bar{b} + \bar{v}\, \sum_{i=0}^{k-1} \bar{\bar{u}}^i \qquad k \in \mathbf{N}. \end{array} \right. \tag{11}$$

Therefore, the invariance relation for the wavelet transform of the self-affine function 8 is

$$(Wf)(\bar{\bar{s}},\bar{b}) = (Wf)(\bar{\bar{s}}^{(k)},\bar{b}^{(k)}). \tag{12}$$

The action of the new operator $U(\bar{\bar{s}}^{(k)},\bar{b}^{(k)})$ with respect to index k defines a "multi-resolution representation" of the function f where all the nested subspaces are translated and scaled versions of each other. The construction of such a multi-resolution scheme for an arbitrary self-affine attractor as defined in section 3.2 is possible and is equivalent to finding the operator $T(\bar{\bar{u}},\bar{v})$. A demonstration of this construction is given in section 4, where the wavelet maxima bifurcation representation is introduced to accomplish this.

4. RECOVERY OF THE SCALING PARAMETERS FROM THE WAVELET TRANSFORM BIFURCATION REPRESENTATION

We will use wavelets with m vanishing moments,[§] see Eq. (7). This will allow us to perform filtering off of the polynomial behaviour of the $m-1$ order according to

$$(W)(D^{(m)} f(x)) = |\bar{\bar{s}}|^{-m}\; (W^{(m)})(f(x)), \tag{13}$$

where the operator $D^{(m)} = d^m/dx^m$ and $W^{(m)}f$ the wavelet transform using a wavelet with m vanishing moments.

The self-affine function can generally be described by a finite set of n affine transformations (compare section 2, Eq. (4)) of the generic form:

$$\left\{ \begin{array}{lcl} \bar{x}' & = & S_{xn}(\bar{x}) \\ y(\bar{x}') & = & \alpha_n\, y(\bar{x}) + \gamma_{n1}\, x_1 + \gamma_{n2}\, x_2 + \delta_n\, . \end{array} \right. \tag{14}$$

If by taking the wavelet transform of y with the wavelet with the appropriate number (in this case at least 2) of vanishing moments, additional components in Eq. (14) are removed, the following invariance relation holds with respect to the affine operator S_{xn}:

$$D_x^{(m)}\, y(\bar{x}') = D_x^{(m)}\, y(S_{xn}(\bar{x})) = \sigma_n^{-m} \alpha_n\, D_x^{(m)}\, y(\bar{x}, \qquad m >= 2\, . \tag{15}$$

As already shown in the previous section, Eq. (12), for $T(\bar{\bar{u}}_n,\bar{v}_n) = S_{xn}$ this invariance reflects (up to the multiplicative factor) in the wavelet transform coefficients:

$$w_D(\sigma_n)\; (W^{(m)}y)(T(\bar{\bar{u}}_n,\bar{v}_n)\; (,)) = \sigma_n^{-m}\alpha_n\; (W^{(m)}y)(,), \;\; m >= 2\, . \tag{16}$$

The factor $w_D(\sigma_n) = {\sigma_n}^{2-D}$ corrects for the possibly fractional support of the attractor, the fractal dimension D of the support can be estimated in the usual way: $\sum_n {\sigma_n}^D = 1$.

It is therefore the second (or higher) derivative of the wavelet transform $W^{(2)}(y)$, which, for the generic self-affine attractor defined by Eq. (4), involves the invariance with respect

[§] In this communication we used an example with no is equivalent to both $\gamma_n = 0$ and $\delta_n = 0$. Therefore, orthogonality of the wavelet to polynomials would not be essential and the wavelet with $m = 0$ could be used. Nevertheless, in the formal considerations we will, however, retain generality.

to the transformation S_{xn} on the coordinates x_1 and x_2, and the multiplicative dependence on the parameters α_n, and will allow the recovery of the parameters of S_{xn} and the α_n's.

What is needed for this purpose is the representation capturing the invariance present in the wavelet transform of the function and allowing the solution of the Eq. (15) through the comparison of related points in $W^{(m)}(y(,))$, Eq. (16). This is achieved in the wavelet transform maxima bifurcation representation.

Once the invariant representation is established the remaining parameters can be recovered from $W^{(1)}(y(,))$ and $W^{(0)}(y(,))$ sampled with the invariant grid of bifurcations[1].

4.1 Wavelet transform local maxima bifurcation representation

We will not go beyond being very brief on the arguments for the construction of the bifurcation representation, referring the reader to earlier publications[1,2] for more details.

Indeed, neither the continuous wavelet transform nor the orthogonal discrete version can achieve the kind of multi-resolution analysis we require. While the continuous version maps all the scale-space relationship originally present in the analysed function onto the scale-space domain in the most redundant way, leaving the invariance which has been sought un-discriminated, the discrete one represents it in an orthogonal fashion on an 'a priori' defined grid, which in general is not 'compatible' with the invariance of the function.

The wavelet transform maxima bifurcation representation was, therefore, derived from the (modulus) maxima representation of Mallat[5]. The particularly convenient feature of Mallat's maxima representation is its translation invariance, which is of great importance in pattern recognition problems. Since fractal functions are a special class of functions where the translation invariance is accompanied by scale invariance, we used unique 'landmarks' in the form of bifurcations of maxima lines to derive scale invariant representation from the maxima lines.

The necessary condition for the local extrema of the wavelet transform $Wf(s, x_1, x_2)$ of the function of two variables $f(x_1, x_2)$ is zero of the partial derivatives:

$$\left\{ \begin{array}{lcl} \frac{d(Wf)(s,x_1,x_2)}{dx_1} & = & 0 \\ \frac{d(Wf)(s,x_1,x_2)}{dx_2} & = & 0\,, \end{array} \right. \tag{17}$$

which points are further classified according to the sufficient condition for local extrema:

$$\left\{ \begin{array}{lcl} \mathcal{H}(s, x_1, x_2) & > & 0 \\ \frac{d^2(Wf)(s,x_1,x_2)}{dx_1^2} & < & 0 \;(> 0) \quad \text{in the case of a local maximum (minimum)} \end{array} \right. \tag{18}$$

where $\mathcal{H}(,,)$ is the Hessian $\mathcal{H}(,,) = D^{(2)}_{x_1{}^2}(Wf)(,,)\; D^{(2)}_{x_1{}^2}(Wf)(,,) - \left(D^{(2)}_{x_1,x_2}(Wf)(,,)\right)^2$.

The bifurcation case is defined by:

$$\left\{ \begin{array}{lcl} Eq.\ (17) & & \\ \mathcal{H}(s, x_1, x_2) & = & 0\,. \end{array} \right. \tag{19}$$

The tree structure apparent in the maxima representation serves as basis for the parameter recovery algorithm utilised in the solution to the IFP. The tree construction is similar to that described in our communication on the one-dimensional case[1]. The expansion of the attractor in scale thus achieved, gives direct insight into the action of the transformation,

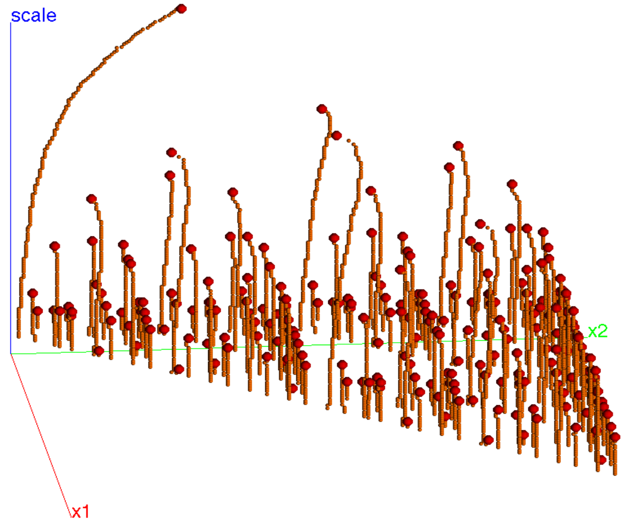

Figure 2: Local maxima of the wavelet transform with associated bifurcations for the example from figure 1. The wavelet used is the Gaussian, $m = 0$.

in this case IFS, used to create the attractor. The 'stages of construction' are therefore revealed and linked with one another in the bifurcation representation.

The next crucial step comprises the finding of the invariance of the bifurcation representation. This can be done by means of tree matching, see Ref.[1]. where the invariance of the representation is sought in the optimal match of the tree to its branches. From the match of pairs of bifurcations found invariant, the parameters of Eq. (16) are estimated.

Space limits prevent elaboration on the procedure and we will restrict ourselves to presenting and interpreting the results for the given example. The affine maps $x_{\{1,2\}} = f(x'_1, x'_2)$ representing scaling and translation parameters of S_{xn} as shown in figure 3. As expected from the diagonal character of S_{xn} for the Sierpiński triangle the linear dependence with consistent slope $1/\sigma_n = 1/0.5$ shows in only one of the coordinates. The translation components are directly visible in the histogram in the figure 4 and the repartition of measure can be verified from the modes of parameter α_n in the upper right of this figure.

5. ACKNOWLEDGEMENTS

Gratitude is expressed to Dr E.H. Dooijes for careful reading and suggestions for improvements to the manuscript. This project is supported by the Dutch Foundation for Scientific Research (NWO-SION).

6. REFERENCES

1. Z.R. Struzik, *Fractals* **3** (1995) (in print).
2. Z.R. Struzik, E.H. Dooijes, F.C.A. Groen, in *Fractal '95, Fractals in the Natural and Applied Sciences*, Ed. M.M. Novak, Chapman & Hall, (in print).
3. M.F. Barnsley, *Fractals Everywhere*, Academic Press, NY, (1988).
4. K. Falconer, *Fractal Geometry - Mathematical Foundations and Applications*, John Wiley (1990).
5. S.G. Mallat, S. Zhong, *IEEE Trans. PAMI* **14**, 710-732 (1992).

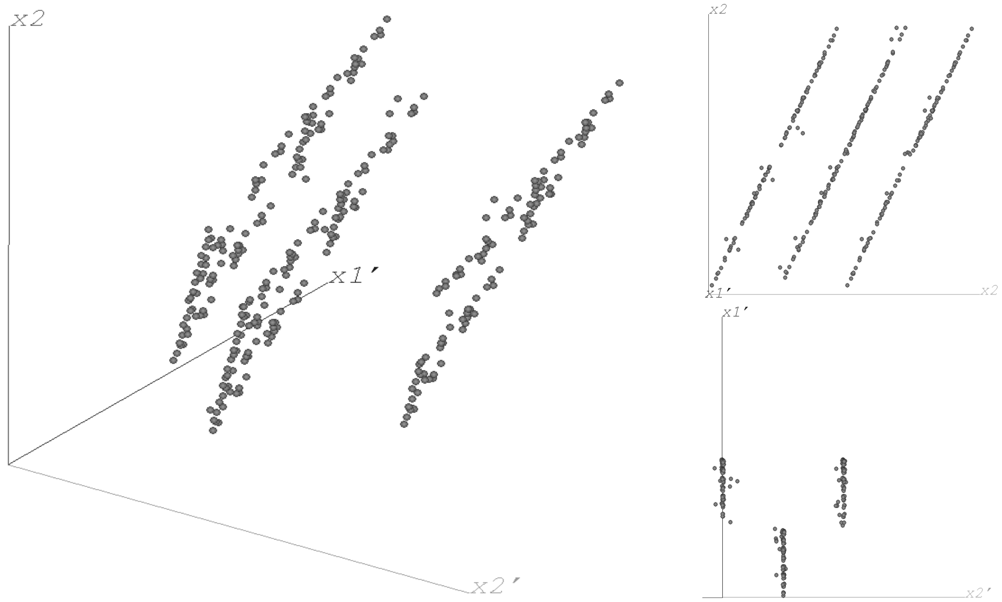

Figure 3: The maps recovered from matching the bifurcations in the representation in figure 2. Of the total of six two-dimensional maps three maps $x_2 = f(x_1', x_2')$ are shown in the figure on the leftmost. The Sierpiński triangle was rotated in order to disconnect the maps. The projection along x_1' in the upper right shows consistent slope of $1/\sigma_n = 1/0.5$ rate with respect to x_2' for all three maps displayed. As expected from the diagonal S_{xn} for the Sierpiński triangle, the linear dependence shows in only one of the coordinates, which is confirmed in the projection in the bottom right figure.

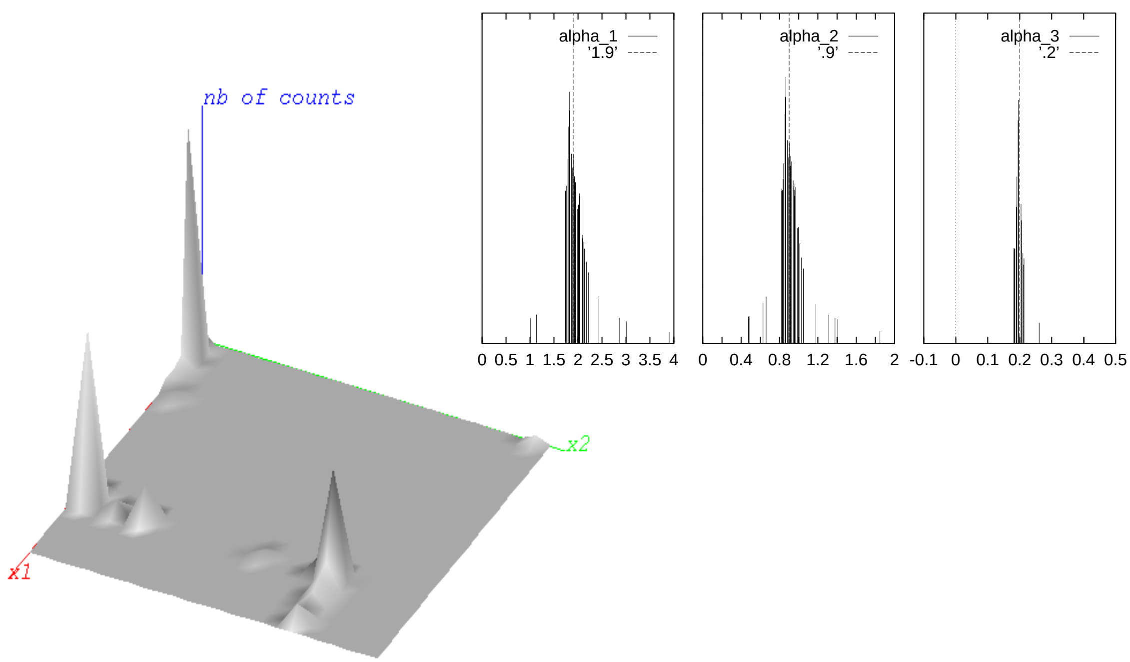

Figure 4: The histogram of the parameters e_n and f_n shows the location of the peaks on a triangle corresponding with the translation vectors of the Sierpiński triangle (left). The modes of the parameter α_n responsible for the distribution of the measure on the triangle (right) show remarkable agreement with the true values.